

Coordination Chemistry of Diselenophosphinate Complexes: The X-ray Single-Crystal Structures of $[K(Se_2PPh_2)(THF)_2]_2$ and $[In(Se_2PPh_2)_3] \cdot L$ ($L = THF, PhMe$)

Robert P. Davies,* Claire V. Francis, Andrew P. S. Jurd, M. Giovanna Martinelli, Andrew J. P. White, and David J. Williams

Department of Chemistry, Imperial College London, South Kensington, London SW7 2AZ, U.K.

Received April 2, 2004

Reaction of potassium diphenylphosphide with elemental selenium is shown to give $[K(Se_2PPh_2)(THF)_2]_2$ **1**, which further reacts with $InCl_3$ to yield $[In(Se_2PPh_2)_3]$ **2**. Crystallization of **2** from either THF or PhMe gave **2**·THF or **2**·PhMe, respectively, both of which form loosely linked dimers in the solid state via Se···Se intermolecular van der Waals interactions. Decomposition of **2** has been studied by TGA.

The chemistry of metal selenolates is of topical interest, due in part to their potential use as single-source precursors to binary and ternary metal chalcogenides.¹ Within this area, we have recently been interested in the synthesis and coordination chemistry of chalcogeno–phosphorus ligand systems, and have published of late on the synthesis of lithium selenophosphinite, diselenophosphinate, and triselenophosphonate complexes.² These seleno–phosphorus ligands were shown to be more stable, easier to handle, and far less pungent than alkyl and aryl selenolates.^{2,3} This has now led us to look at the synthesis and characterization of other main group metal complexes of these ligands.

The indium(III) complexes of seleno–phosphorus ligands are of particular interest to us due to their potential application as single-source precursors to indium selenide thin films and quantum dots. Precedent to these applications lies in the reported use of dithiophosphinate and phosphino-chalcogenoamidate complexes such as $[Cd(S_2PR_2)_2]$ ($R = CH_3$,⁴ C_2H_5 ⁵) and $[M\{tBu_2P(Se)NR\}_2]$ ($M = Zn, Cd, Cr$,

Mn, Fe, Co ; $R = iPr, c-C_6H_{11}$)⁶ for the growth of semi-conducting metal chalcogenide thin films using chemical vapor deposition (CVD) processes, and in the recently reported effectiveness of imino–bis(diisopropylphosphine selenide) complexes, e.g., $Cd[N(SeP*i*Pr_2)_2]_2$, as reagents for the one-step synthesis of metal selenide quantum dots.⁷ In addition, although dithiophosphinate complexes of main group metals are well-known,⁸ there are very few structurally characterized main group metal complexes of the homologous diselenophosphinates or diselenophosphates, the only examples being the alkali metal complexes $[Ph_2PSe_2Li \cdot THF \cdot TMEDA]_2$ [$TMEDA = \{(CH_3)_2NCH_2\}_2$], $[Na_2(Se_2PPh_2)_2 \cdot THF \cdot 5H_2O]$,⁹ and $[K_2(PhPSe_2)_2CH_2]^{10}$

Potassium diselenophosphinate $[K(Se_2PPh_2)(THF)_2]_2$ **1** was obtained in 79% yield from the reaction of potassium diphenylphosphide with 2 equiv of gray selenium powder in THF/toluene (Scheme 1).

Scheme 1



X-ray diffraction studies¹¹ show **1** to crystallize as discrete centrosymmetric dimers with a central $K_2P_2Se_4$ cage bounded by phenyl and THF units (Figure 1). The P–Se bond lengths of 2.132(2) Å [Se(1)] and 2.150(2) Å [Se(2)] are intermediate between those expected for P–Se single (2.26 Å)² and double (2.09 Å)¹² bonds, indicative of delocalization of the negative charge across the PSe_2 unit and a P–Se bond order of 1.5.

* To whom correspondence should be addressed. E-mail: r.davies@imperial.ac.uk.

- (1) (a) Singh, H. B.; Sudha, N. *Polyhedron* **1996**, *15*, 745–763. (b) Arnold, J. In *Progress in Inorganic Chemistry*; Karlin, K. D., Ed.; Wiley: New York, 1995; Vol. 43, pp 353–418. (c) Gleizes, A. N. *Chem. Vap. Deposition* **2000**, *6*, 155–173. (d) Bochmann, M. *Chem. Vap. Deposition* **1996**, *2*, 85–96. (e) Lazell, M.; O'Brien, P.; Otway, D. J.; Park, J.-H. *J. Chem. Soc., Dalton Trans.* **2000**, 4479–4486.
- (2) Davies, R. P.; Martinelli, M. G. *Inorg. Chem.* **2002**, *41*, 348–352.
- (3) Clegg, W.; Davies, R. P.; Snaith, R.; Wheatley, A. E. H. *Eur. J. Inorg. Chem.* **2001**, 1411–1413.
- (4) Takahashi, Y.; Yuki, R.; Sugiyama, M.; Motojima, S.; Sugiyama, K. *J. Cryst. Growth* **1980**, *50*, 491–497.
- (5) Evans, M. A. H.; Williams, J. O. *Thin Solid Films* **1982**, *87*, L1–L2.

- (6) (a) Bwembya, G. C.; Song, X.; Bochmann, M. *Chem. Vap. Deposition* **1995**, *1*, 78. (b) Song, X.; Bochmann, M. *J. Chem. Soc., Dalton Trans.* **1997**, 2689–2692.
- (7) Crouch, D. J.; O'Brien, P.; Malik, M. A.; Skabara, P. J.; Wright, S. P. *Chem. Commun.* **2003**, 1454–1455.
- (8) (a) Haiduc, I. *J. Organomet. Chem.* **2001**, *623*, 29–42. (b) Walther, B. *Coord. Chem. Rev.* **1984**, *60*, 67–105. (c) Mehrotra, R. C.; Srivastava, G.; Chauhan, B. P. S. *Coord. Chem. Rev.* **1984**, *55*, 207–259.
- (9) Pilkington, M. J.; Slawin, A. M. Z.; Williams, D. J.; Woollings, J. D. *Polyhedron* **1991**, *10*, 2641–2645.
- (10) Kilian, P.; Bhattacharyya, P.; Slawin, A. M. Z.; Woollings, J. D. *Eur. J. Inorg. Chem.* **2003**, 1461–1467.

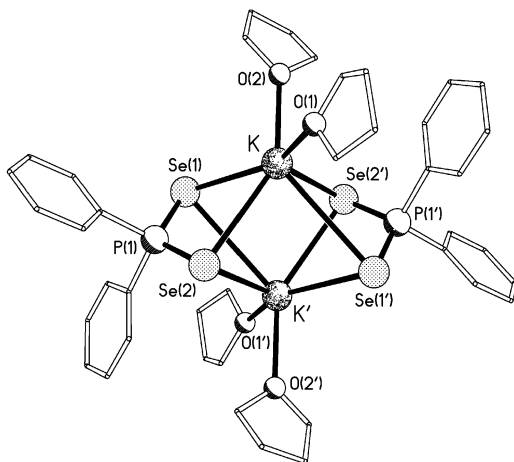


Figure 1. Molecular structure of $[K(Se_2PPh_2)(THF)_2]_2$ **1**.

This delocalization can also be observed in solution using ^{31}P NMR spectroscopy from the $^1J_{PSe}$ coupling constant (-642 Hz) which is midway between expected values for single (-200 to -600 Hz) and double (-800 to -1200 Hz) P–Se bonds.¹³ The infrared spectrum of a Nujol mull of **1** shows strong absorptions at 561 and 490 cm^{-1} which can be ascribed to the asymmetric (ν_{as}) and symmetric (ν_s) stretching vibrations of the PSe_2 groups. The solid-state structure reveals the diselenophosphinate ligands in **1** to bridge the two potassium centers in a $\mu_2\text{-}\eta^2, \eta^2$ mode with each Ph_2PSe_2 ligand coordinating in an isobidentate (symmetric) fashion to one potassium center and anisobidentately (asymmetrically) to the other. This results in a distorted K_2Se_4 octahedral core, with three short K–Se contact distances [K–Se(1) $3.402(2)$ Å, K–Se(2) $3.431(2)$ Å, K–Se(2') $3.378(3)$ Å] and one long one [K–Se(1') $3.913(3)$ Å]. There are no significant interdimer interactions.

Metathesis reactions of **1** with $InCl_3$ gave the tris-(diselenophosphinato)indium complex $[In(Se_2PPh_2)_3]$ **2**, which was crystallized from toluene/THF to yield yellow prisms of **2**·THF (46% yield), and from toluene in the absence of THF to give yellow needles of **2**·PhMe (40% yield). Unlike the crystals of **1**, those of **2**·THF were observed to be air

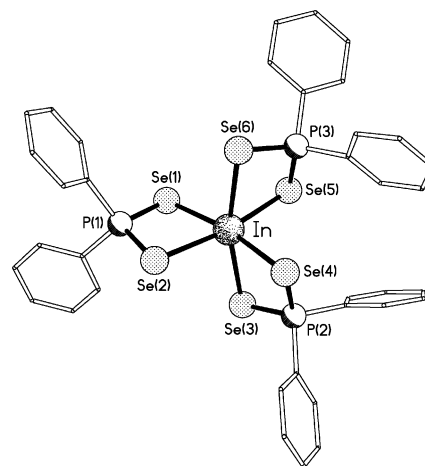


Figure 2. Molecular structure of the $[In(Se_2PPh_2)_3]$ complex in **2**·THF. Though a molecule with a Δ configuration is shown, the crystals of both **2**·THF and **2**·PhMe are racemic and there are equal numbers of Δ and Λ forms present.

and moisture stable, showing no discernible decomposition (using 1H and ^{31}P NMR spectroscopy) over a period of six weeks when left open to the atmosphere. Single-crystal X-ray analysis¹¹ of both **2**·THF and **2**·PhMe revealed (Figure 2) a pair of structures with isostructural $[In(Se_2PPh_2)_3]$ units (rms deviation 0.13 Å for the P_3Se_6In core) and an included solvent molecule. In each case the diselenophosphinate ligands coordinate in an approximate isobidentate fashion, forming four-membered Se–P–Se–In chelate rings with In–Se distances in the range $2.6992(12)$ – $2.7782(13)$ Å for **2**·THF [$2.7181(12)$ – $2.7986(12)$ Å for **2**·PhMe] and P–Se distances in the range $2.168(3)$ – $2.180(3)$ Å [$2.163(3)$ – $2.187(3)$ Å]. Though slightly longer than seen in **1**, these P–Se distances are again indicative of a bond order of ca. 1.5. This is also reflected in the $^1J_{PSe}$ (^{31}P NMR) coupling constant of -649 Hz, and in the infrared asymmetric and symmetric bond stretches at 534 and 445 cm^{-1} . The geometry at the indium center is trigonally distorted octahedral as a consequence of the restricted bite, $80.05(4)$ – $80.18(3)^\circ$ [$79.58(3)$ – $80.90(3)^\circ$], of the chelating diselenophosphinate ligand with the trans Se–In–Se bond angles in the range $164.83(4)$ – $170.40(4)^\circ$ [$161.74(4)$ – $171.33(4)^\circ$]. The structures of the $[In(Se_2PPh_2)_3]$ unit in **2**·THF and **2**·PhMe are therefore similar to that reported for the sulfur homologue $[In(S_2PPh_2)_3]$,¹⁴ although the more restricted bite of the dithiophosphinate ligand (av 77.9° cf. av 80.2° for the seleno species) leads to a greater trigonal distortion of the geometry at the metal center. However, in contrast to $[In(S_2PPh_2)_3]$, **2**·THF and **2**·PhMe both show a packing motif with dimerization between centrosymmetrically related $[In(Se_2PPh_2)_3]$ units occurring via noncovalent Se \cdots Se interactions (Figure 3). Though the basic motif is the same, the Se \cdots Se contact distances for the two solvates of **2** differ markedly. In **2**·THF only one of the Se \cdots Se separations [$3.8145(14)$ Å] is noticeably less than the sum of the van der Waals radii (4.0 Å), and thus falls within the range of previously reported intermolecular nonbonding Se \cdots Se distances (3.3 – 3.9 Å),¹⁵

(11) Crystal data for **1**: $C_{40}H_{52}K_2O_4P_2Se_4$, $M = 1052.80$, $P2_1/n$ (No. 14), $a = 10.2778(8)$ Å, $b = 17.8297(13)$ Å, $c = 12.8935(16)$ Å, $\beta = 93.158(8)^\circ$, $V = 2359.1(4)$ Å³, $Z = 2$ (C_i symmetry), $\rho_{calcd} = 1.482$ g cm^{-3} , $\mu(Mo K\alpha) = 3.390$ mm⁻¹, $T = 233$ K, colorless prisms; 4137 independent measured reflections, $R_1 = 0.062$, $wR_2 = 0.129$, 1985 independent observed absorption corrected reflections [$|F_o| > 4\sigma(|F_o|)$], $2\theta_{max} = 50^\circ$, 265 parameters. For **2**·THF: $C_{36}H_{30}P_3Se_6In \cdot C_4H_8O$, $M = 1216.19$, $P2_1/n$ (No. 14), $a = 13.1962(10)$ Å, $b = 15.2780(15)$ Å, $c = 21.780(3)$ Å, $\beta = 94.606(8)^\circ$, $V = 4376.9(7)$ Å³, $Z = 4$, $\rho_{calcd} = 1.846$ g cm^{-3} , $\mu(Mo K\alpha) = 5.669$ mm⁻¹, $T = 293$ K, yellow prisms; 7666 independent measured reflections, $R_1 = 0.055$, $wR_2 = 0.099$, 4539 independent observed absorption corrected reflections [$|F_o| > 4\sigma(|F_o|)$], $2\theta_{max} = 50^\circ$, 408 parameters. For **2**·PhMe: $C_{36}H_{30}P_3Se_6In \cdot C_7H_8$, $M = 1236.22$, $P2_1/n$ (No. 14), $a = 12.8500(15)$ Å, $b = 15.427(2)$ Å, $c = 22.395(2)$ Å, $\beta = 98.512(9)^\circ$, $V = 4390.6(8)$ Å³, $Z = 4$, $\rho_{calcd} = 1.870$ g cm^{-3} , $\mu(Mo K\alpha) = 5.652$ mm⁻¹, $T = 183$ K, yellow needles; 5738 independent measured reflections, $R_1 = 0.047$, $wR_2 = 0.079$, 3907 independent observed absorption corrected reflections [$|F_o| > 4\sigma(|F_o|)$], $2\theta_{max} = 45^\circ$, 396 parameters.

(12) *Handbook of Chemistry and Physics*, 75th ed.; Lide, D. R., Ed.; CRC Press: Boca Raton, FL, 1995; pp 9–12.

(13) (a) Duddeck, H. In *Encyclopedia of Nuclear Magnetic Resonance*; Grant, D. M., Harris, R. K., Eds.; Wiley: New York, 1996; Vol 7, pp 4623–4635. (b) Duddeck, H. *Prog. Nucl. Magn. Reson. Spectrosc.* **1995**, *27*, 1–323.

(14) Zuckerman-Schpector, J.; Haiduc, I.; Silvestru, C.; Cea-Olivares, R. *Polyhedron* **1995**, *14*, 3087–3094.

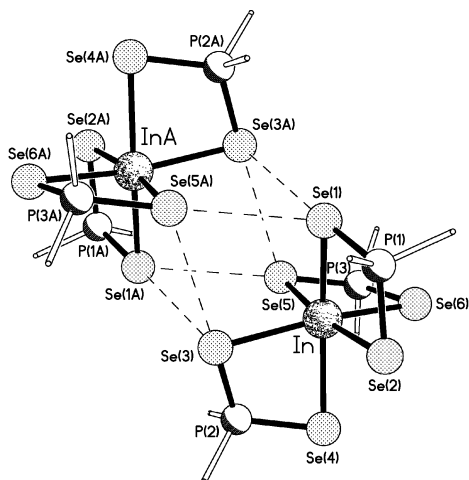


Figure 3. Dimerization via intermolecular nonbonding Se...Se interactions in **2-PhMe** (the phenyl rings have been omitted for clarity).

Table 1. Intermolecular Distances (Å) and Angles (deg) for **2-THF** and **2-PhMe**

	2-THF	2-PhMe
Se(1)···Se(3A)	3.8145(14)	3.5340(14)
Se(3)···Se(5A)	4.334(2)	3.7958(14)
Se(1)···Se(5A)	4.007(2)	3.7234(14)
P(1)–Se(1)···Se(3A)	160.96(8)	173.79(7)
P(1)–Se(1)···Se(5A)	108.96(9)	113.78(8)
P(2)–Se(3)···Se(1A)	113.03(7)	106.24(7)
P(2)–Se(3)···Se(5A)	169.59(8)	173.45(7)
P(3)–Se(5)···Se(1A)	177.37(8)	173.36(8)
P(3)–Se(5)···Se(3A)	123.09(8)	118.29(8)

whereas in **2-PhMe** the Se...Se contacts range between 3.5340(14) and 3.7958(14) Å (Table 1). Such nonbonding Se...Se interactions are well-known and have found utility in crystal engineering, for example in the formation of tubular structures from the columnar stacking of chalcogen containing macrocyclics.¹⁵ In contrast to **2-THF** and **2-PhMe**, the closest intermolecular S...S separation in the structure of [In(S₂PPh₂)₃] is 4.40 Å.¹⁴

Previous quantum chemical model calculations have shown the so-called nonbonding chalcogen–chalcogen intermolecular interactions in chalcogenoethers (R₂X; X = S, Se, Te) to arise due to interaction of the occupied *np* orbital on the chalcogen of a R₂X molecule with the empty σ^* orbital of the R–X bond of an adjacent R₂X molecule (Figure 4a).^{15,16} This results ideally in a linear RX...X interaction ($\theta_1 = 180^\circ$) perpendicular to one of the chalcogenoether groups ($\theta_2 = 90^\circ$). Inspection of the intermolecular interactions in **2-THF** and **2-PhMe** reveals that similar interactions may well be occurring between the Se 4p or π orbital on one diselenophosphate ligand and the P–Se σ^* orbital of an adjacent diselenophosphate (Figure 4b), with θ_1 values observed in the range 160.96(8)–173.79(7)° and θ_2 values in the range 106.24(7)–118.29(8)° (Table 1). In **2-THF** one selenium [Se(3)] on each complex would therefore be acting

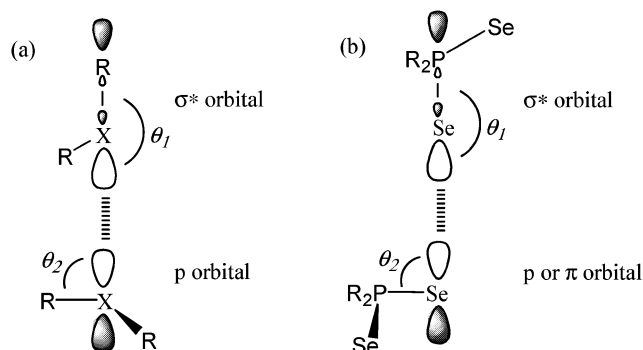


Figure 4. Interaction of the occupied p orbitals with the empty σ^* orbitals in (a) chalcogenoethers and (b) **2-THF** and **2-PhMe**.

as a donor and one [Se(1)] as an acceptor; however, in **2-PhMe** each complex contains three seleniums [Se(1), Se(3), and Se(5)] which act as both donors and acceptors (similar dual donor and acceptor behavior has been reported for chalcogenoethers¹⁵).

In order to study the decomposition pathway of **2** and to evaluate its potential use as a single-source precursor for In₂Se₃, TGA (10 °C min⁻¹, 20–500 °C, under N₂) was carried out on **2-THF**. A small weight loss was observed for **2-THF** in the range 85–125 °C, attributable to the loss of lattice THF, and a more significant weight loss of 75.2% from 375 to 450 °C, attributable to decomposition of **2** to In₂Se₃ (calculated weight loss of 79.6% for In₂Se₃ formation from **2**). Elemental analysis on the decomposition product is consistent with its assignment as In₂Se₃, showing no major contamination by carbon, hydrogen, or phosphorus (C, H, P found <0.5%). The air and moisture stability of **2**, its facile synthesis, and its lack of a pungent odor give it several advantages in terms of ease of use over existing indium selenide single-source precursors such as air-sensitive and noxious alkylindium selenolates [e.g., In(SePh)₃ and Me₂In(SePh)]¹⁷ and indium selenocarbamates In(Se₂CNR¹R²)₃ which, although excellent air-stable precursors, need to be prepared from toxic and noxious carbon diselenide.¹⁸ More detailed studies on the utility of **2** as a single-source precursor toward thin films and nanoclusters are currently being undertaken.

Acknowledgment. This work was supported by a studentship from the Department of Chemistry, Imperial College, London (M.G.M.), a CRF grant from the University of London, and a Royal Society Research Grant.

Supporting Information Available: Three X-ray crystallographic files in CIF format, full experimental details for all compounds, and the TGA plot for **2-THF**. This material is available free of charge via the Internet at <http://pubs.acs.org>.

IC049567X

(15) Gleiter, R.; Werz, D. B.; Rausch, B. J. *Chem. Eur. J.* **2003**, *9*, 2676–2683.

(16) Werz, D. B.; Rausch, B. J.; Gleiter, R. *Tetrahedron Lett.* **2002**, *43*, 5767–5769.

(17) Gysling, H. J.; Wernburg, A. A. *Chem. Mater.* **1992**, *4*, 900–905.

(18) (a) Ludolph, B.; Mailk, M. A.; O'Brien, P.; Revaprasadu, N. *Chem. Commun.* **1998**, 1849–1850. (b) Revaprasadu, N.; Malik, M. A.; O'Brien, P.; Zulu, M. M.; Wakefield, M. *J. Mater. Chem.* **1998**, *8*, 1885–1888.